

1 **N₂ fixation in eddies of the eastern tropical South Pacific Ocean**

2

3 C. R. Löscher^{1,2*}, A. Bourbonnais³, J. Dekaezemacker^{4,5}, Chawalit N. Charoenpong^{6,7}, M. A. Altabet³, H.
4 W. Bange^{1,8}, R. Czeschel¹, C. Hoffmann², R. Schmitz²

5

6 [1] {Helmholtz Center for Ocean Research Kiel, Düsternbrooker Weg 20 24105 Kiel, Germany}

7 [2] {Institute of Microbiology, Christian Albrechts University of Kiel, Am Botanischen Garten 1-9, 24118
8 Kiel, Germany}

9 [3] {School for Marine Science and Technology, University of Massachusetts Dartmouth, New Bedford,
10 Massachusetts, USA}

11 [4] {Department of Biogeochemistry, Max Planck Institute for Marine Microbiology, Celsiusstraße 1,
12 28359 Bremen, Germany}

13 [5] {now at: MARUM, University of Bremen, 28359 Bremen, Germany - Helmholtz Young Investigator
14 Group SEAPUMP, Alfred Wegener Institute for Polar and Marine Research, 27570 Bremerhaven,
15 Germany}

16 [6] {Department of Marine Chemistry and Geochemistry, Woods Hole Oceanographic Institution, Woods
17 Hole, Massachusetts, USA}

18 [7] {Department of Earth, Atmospheric and Planetary Sciences, Massachusetts Institute of Technology,
19 Cambridge, Massachusetts, USA}

20 [8] {Christian-Albrechts-Universität zu Kiel, Kiel, Germany}

21

22 *Correspondence to: C. Löscher (cloescher@geomar.de)

23

24 Short title: N₂ fixation in ETSP eddies

25

26 **Abstract**

27 Mesoscale eddies play a major role in controlling ocean biogeochemistry. By impacting nutrient
28 availability and water column ventilation, they are of critical importance for oceanic primary production.
29 In the eastern tropical South Pacific Ocean off Peru, where a large and persistent oxygen deficient zone is
30 present, mesoscale processes have been reported to occur frequently. However, investigations on their
31 biological activity are mostly based on model simulations, and direct measurements of carbon and
32 dinitrogen (N_2) fixation are scarce.

33 We examined an open ocean cyclonic eddy and two anticyclonic mode water eddies: a coastal one and an
34 open ocean one in the waters off Peru along a section at $16^\circ S$ in austral summer 2012. Molecular data and
35 bioassay incubations point towards a difference between the active diazotrophic communities present in
36 the cyclonic eddy and the anticyclonic mode water eddies.

37 In the cyclonic eddy, highest rates of N_2 fixation were measured in surface waters but no N_2 fixation
38 signal was detected at intermediate water depths. In contrast, both anticyclonic mode water eddies showed
39 pronounced maxima in N_2 fixation below the euphotic zone as evidenced by rate measurements and
40 geochemical data. N_2 fixation and carbon (C) fixation were higher in the young coastal mode water eddy
41 compared to the older offshore mode water eddy. A co-occurrence between N_2 fixation and biogenic N_2 ,
42 an indicator for N loss, indicated a link between N loss and N_2 fixation in the mode water eddies, which
43 was not observed for the cyclonic eddy. The comparison of two consecutive surveys of the coastal mode
44 water eddy in November 2012 and December 2012 revealed also a reduction of N_2 and C fixation at
45 intermediate depths along with a reduction in chlorophyll by half, mirroring an aging effect in this eddy.
46 Our data indicate an important role for anticyclonic mode water eddies in stimulating N_2 fixation and thus
47 supplying N offshore.

48 1 Introduction

49 **Reactive nitrogen (N) limits** primary production in large parts of the ocean (Codispoti, 1989). Biological
50 dinitrogen (N₂) fixation is an important external input of N, representing more than 60-80% of the new N
51 provided to the Ocean (Codispoti, 2007;Duce et al., 2008), and can partially relieve N limitation. For
52 decades, N₂ fixation was conventionally thought to occur mainly in nutrient-depleted surface waters such
53 as found in the subtropical gyres (Sohm et al., 2011). However, some recent modeling studies have
54 suggested a close spatial link between fixed N loss, i.e. N₂ production via anammox and/or denitrification,
55 occurring in oxygen deficient zones (ODZs), and N₂ fixation taking place in the adjacent surface ocean
56 with the consequence that the potential habitat of N₂ fixing organisms is larger than previously thought
57 (Deutsch et al., 2007). Furthermore, as both processes are favored under oxygen depleted conditions and
58 as some organisms responsible for these processes do not need light, their coupling in ODZ waters would
59 damp excursions in the oceanic N inventory and promote stability of the global N budget.

60 In the recent years, efforts have been placed on investigating N₂ fixation in the eastern tropical South
61 Pacific (ETSP) (Dekaezemaker et al., 2013;Fernandez et al., 2015;Löscher et al., 2014) and the results of
62 those field studies have significantly advanced our understanding of diazotrophy in low-O₂ regions of the
63 ocean. They indeed confirmed the frequent occurrence of N₂ fixation in denitrified waters and below the
64 euphotic zone. A biogeochemical significance of non-cyanobacterial diazotrophs (i.e., microbes capable of
65 N₂ fixation) has been described, and their enormous potential to fix N₂ in the ETSP seems also to depend
66 on organic matter supply (Fernandez et al., 2015).

67 **In addition to its remarkable biological activities, the physically dynamic character of the ETSP in the**
68 **upwelling system off Peru favors mesoscale activities (Chelton et al., 2011). Compared to other upwelling**
69 **regions (e.g. off California, Benguela) enhanced frequency of eddies has been reported for this region**
70 **(Chaigneau et al., 2009).** Mesoscale eddies are physical structures with horizontal scales of less than 100
71 km and timescales of around one month. These features can transport physical and chemical properties
72 from the coast towards the open ocean (Klein and Lapeyre, 2009) and impact on the ocean by modulating
73 nutrient availability (Fong et al., 2008;Altabet et al., 2012). Cyclonic and mode water eddies can inject
74 nutrients to the euphotic zone through vertical displacement of isopycnal surfaces, which increases surface
75 primary production (McGillicuddy et al., 2007). Overall, investigations on the impact of mesoscale eddies
76 on N₂ fixation are scarce. Fong et al. (2008) reported a stimulation of N₂ fixation in a mode water eddy of
77 the oligotrophic North Pacific. Another study showed increased abundances of *Trichodesmium* in
78 mesoscale eddies of the Western South and North Atlantic associated with strong temporal variations
79 (Olson et al., 2015).

80 In the ODZ off Peru, mesoscale eddies have previously been identified as N loss hotspots (Altabet et al.,
81 2012;Bourbonnais et al., 2015), but to date no detailed surveys on their relevance for N₂ fixation in this

82 region are available. The spatial connection between N loss and N₂ fixation that has been proposed for this
83 region (Fernandez et al., 2011) may, however, indicate a potential for N₂ fixation associated to eddies in
84 the ODZ off Peru.

85 The major goal of this study was to advance our understanding of eddy-related N₂ fixation by surveying
86 one cyclonic and two anticyclonic mode water eddies along a 16.45°S transect during the R/V Meteor
87 cruises M90 and M91 in November-December 2012. During the survey of these three eddies, we
88 measured both N₂ fixation rates and abundances of *nifH*, a key functional molecular marker gene.
89 Additionally, N₂ fixation was compared to N loss signals in the water column to investigate their coupling
90 in the eddy systems. One particular eddy was surveyed twice (in November 2012 and December 2012),
91 allowing monitoring the temporal development of N₂ fixation and primary production in an aging eddy.

92

93 **2 Material and Methods**

94 2.1 Sampling description and biogeochemical parameters

95 Selection of sampling stations and identification of eddy cores and edges were based on sea level height
96 anomaly data from Aviso (<http://aviso.altimetry.fr>) and followed the criteria defined by Stramma et al.
97 (2013). Briefly, the eddies were tracked during the R/V Meteor cruises M90 and M91 in November-
98 December 2012. Three eddies were detected in area extending from the Peruvian coast to ~84°W and from
99 15°S to 18°S (Fig. 1, Stramma et al., 2013). Two eddies (further referred to as eddy A centered at about
100 16°S, 76°W and eddy B centered in the open ocean at about 17°S, 83°W) were mode water eddies and one
101 was cyclonic (further referred to as eddy C, centered in the open ocean at 16°S, 80°W, Fig. 1). The age of
102 the eddy was determined by Stramma et al. (2013) bases on satellite monitoring of sea level height
103 anomaly data. At the time of the survey, the near-coastal eddy A was about 2 months old (3 months during
104 the second survey), while the open-ocean eddy B was 5 months and the cyclonic open-ocean eddy C was 2
105 months old.

106 Samples for salinity, O₂ concentrations and nutrients (nitrate, NO₃⁻; nitrite, NO₂⁻; phosphate, PO₄³⁻ and
107 ammonium, NH₄⁺) were taken from a 24-Niskin- bottle rosette equipped with a conductivity-temperature-
108 depth (CTD) sensor or from a pump-CTD (Friedrich et al., 1988). O₂ concentrations were determined
109 using a Seabird sensor, calibrated to the Winkler method (precision of 0.45 μmol L⁻¹; the lower detection
110 limit was 2 μmol L⁻¹; (Stramma et al., 2013)). Nutrient concentrations were determined as previously
111 described (Grasshoff, 1999) using a QuAatro auto-analyzer (SEAL Analytical GmbH, Germany;
112 precision for NO₂⁻, NO₃⁻, and PO₄³⁻ were ± 0.1 μmol L⁻¹, ±0.1 μmol L⁻¹, ±0.02 μmol L⁻¹, respectively).
113 Excess PO₄³⁻, P* (i.e., the anomaly in P relative to expected stoichiometry with N) was calculated from

114 dissolved inorganic nitrogen (DIN= $\text{NO}_3^- + \text{NO}_2^-$) and PO_4^{3-} measurements according to Deutsch et al.
115 (2007):

116
$$P^* = \text{PO}_4^{3-} - \text{DIN} / r_{16:1},$$

117 where $r_{16:1}$ is the ratio of nitrate to phosphate at Redfield conditions. Positive P^* has been thought to
118 stimulate N_2 fixation

119

120 2.2 N_2/Ar , Biogenic N_2 measurements

121 High precision measurements of N_2/Ar were made on septum sealed samples using on-line gas extraction
122 system coupled to a multicollector continuous flow-IRMS as described in Charoenpong et al. (2014). N_2
123 excess ($[\text{N}_2]_{\text{excess}}$), i.e. the observed $[\text{N}_2]$ minus the equilibrium $[\text{N}_2]$ at in-situ temperature and salinity, was
124 calculated based on the N_2/Ar ratio with daily calibration against seawater standards equilibrated with air
125 at fixed temperatures (5°C, 15°C and 25°C). Precision (standard deviation) for duplicate measurements
126 was generally better than $\pm 0.7 \mu\text{mol L}^{-1}$ for $[\text{N}_2]_{\text{excess}}$.

127 We calculated biogenic $[\text{N}_2]$ ($[\text{N}_2]_{\text{biogenic}}$), the $[\text{N}_2]$ produced by denitrification or anammox, by subtracting
128 the $[\text{N}_2]_{\text{excess}}$ at a background station ($[\text{N}_2]_{\text{excess_bkgd}}$) unaffected by N loss ($[\text{O}_2] > 10 \mu\text{mol L}^{-1}$) located north
129 of the ODZ (1.67°N, 85.83°W, M90 cruise) from the observed $[\text{N}_2]_{\text{excess}}$ at corresponding σ_θ (as described
130 in Bourbonnais et al., 2015):

131
$$[\text{N}_2]_{\text{excess_bkgd}} (\mu\text{mol L}^{-1}) = 1 \times 10^{-9} e^{0.84\sigma_\theta}$$

132 This corrects for non-local biological N loss as well as physically-produced deviations in equilibrium
133 N_2/Ar (Hamme and Emerson, 2002).

134

135 2.3 N_2/C -fixation rate measurements

136 Sample seawater was taken from the Niskin bottles or from the pump-CTD and filled into 4.5 L
137 polycarbonate bottles (Nalgene, Thermo Fisher, Waltham, Massachusetts, USA) capped with Teflon-
138 coated butyl rubber septum. Incubations were performed as previously described (Grosskopf et al., 2012)
139 with the method developed by Mohr et al. (2010). In contrast to the traditionally used bubble addition
140 method (Montoya et al., 1996), $^{15}\text{N}_2$ gas (Cambridge Isotopes, Lot no.: I-16727) was dissolved in degassed
141 water from the same sampling depth in order to guarantee a high dissolution and a stable enrichment in

142 ¹⁵N₂. Each incubation bottle was supplemented with 100 mL of ¹⁵N₂-enriched seawater containing defined
143 amounts of 98% ¹⁵N₂ gas in order to reach final and constant ¹⁵N₂ enrichment of 2.4 ± 0.144 atom%. A
144 recent study reported a slight potential contamination of ¹⁵N₂ gas with 0.024 ± 0.006 μmoles ¹⁵N-NO₃⁻
145 /NO₂⁻ and 0.014 ± 0.004 μmoles ¹⁵N-NH₄⁺ per mole ¹⁵N₂ (Dabundo et al., 2014). According to Dabundo et
146 al. (2014), however, low concentrations of contaminants in Cambridge-¹⁵N₂ gas do not significantly inflate
147 N₂ fixation rates such as those presented here. In addition, we examined the ¹⁵N₂ gas used in our
148 incubations following the hypobromide oxidation method (Warembourg, 1993) and no contamination has
149 been detected. For each bottle, the initial enrichment of ¹⁵N₂ has been determined and considered for the
150 calculation of the rates.

151 For carbon fixation measurements, NaH¹³CO₃ (98 atom% ¹³C, Sigma-Aldrich, St. Louis, Mo, USA) was
152 dissolved in sterile MilliQ water (1g/ 50 mL). 1 ml was added to the incubations with a syringe (~3.5
153 atom% final in 4.5 L bottles). In order to investigate the contribution of heterotrophic vs. autotrophic
154 diazotrophs to N₂ fixation, glucose addition experiments were performed with ¹³C-labelled glucose
155 (Sigma-Aldrich, St. Louis, Mo, USA), dissolved in MilliQ water (1.44 g L⁻¹), and the concentrated
156 solution was added through the septum with a syringe to yield a final concentration of 2 μmol L⁻¹ glucose.
157 Bottles from surface water were kept in a seawater-cooled on-deck Plexiglas incubators covered with blue
158 light foil (blue-lagoon, Lee filters, Andover, Hampshire, UK) that mimics the ambient irradiance at around
159 10 m depth. Samples from the ODZ were stored at 12°C in the dark. After 24 hours of incubation, 0.7 –
160 2.5 L of seawater were filtered onto pre-combusted (450°C, 5 hours) 25 mm diameter GF/F filters
161 (Whatman, GE healthcare, Chalfont St Gile, UK) under gentle vacuum (-200 mbar). The filtrations were
162 stopped after one hour since high particle load in surface waters often lead to a clogging of the filters.
163 Filters were oven dried (50°C) for 24 hours and stored over desiccant until analysis. Environmental
164 samples of 2 L untreated seawater were filtered and prepared in the same way to serve as blank values for
165 natural abundance. For isotope analysis, GF/F filters were acidified over fuming HCl overnight in a
166 desiccator to remove inorganic C. Filters were then oven-dried for 2 hours at 50°C and pelletized in tin
167 cups. Samples for particulate organic carbon and nitrogen (POC and PON) and isotopic composition were
168 analyzed on an Elemental Analyzer Flash EA 1112 series (Thermo Fisher, Waltham, Massachusetts,
169 USA) coupled to a mass spectrometer (Finnigan Delta Plus XP, Thermo Fisher, Waltham, Massachusetts,
170 USA). Measurements were calibrated using reference gases between each sample and caffeine every 6
171 samples. A table of N₂ and C fixation rate measurements is given in the supplemental material.

172 Possible correlations between environmental parameters and N₂ fixation rates were explored by principal
173 component analysis (PCA) based on 58 cases. Computations were performed in PAST version 3.07
174 (Hammer et al., 2001). Metadatasets for M90 and M91 were deposited at PANGAEA

175 (doi:10.1594/PANGAEA.830245, doi:10.1594/PANGAEA.857751, doi:10.1594/PANGAEA.817193,
176 doi:10.1594/PANGAEA.817174).

177

178 2.4 Molecular methods

179 For molecular analysis, nucleic acid samples were collected by filtering up to 1 L of seawater (exact
180 volumes were recorded and the filtration time was shorter than 20 min) onto polycarbonate membrane
181 filters with a pore size of 0.2 μm (Millipore, Darmstadt, Germany). Immediately after collection, samples
182 were flash frozen in liquid nitrogen and stored at $-80\text{ }^{\circ}\text{C}$ until extraction. Nucleic acids were extracted
183 using DNA/RNA AllPrep Kit (Qiagen, Hildesheim, Germany) with minor changes in the protocol
184 (Löscher et al., 2014).

185 For cDNA library construction, residual DNA was removed from the purified RNA by a DNase I
186 treatment (Life Technologies, Carlsbad, CA, USA). The extracted RNA was gene specifically reverse
187 transcribed to cDNA using the Superscript III First Strand synthesis Kit (Life Technologies, Carlsbad, CA,
188 USA) following the manufacturers' protocol and *nifH* cluster specific no-template qPCRs were performed
189 to assure the purity of RNA. Quantitative PCRs were performed with cDNA as described, before (Löscher
190 et al., 2014); however, a ViiA7 qPCR system (Life Technologies, Carlsbad, CA, USA) was used and the
191 reaction volume was reduced to 12.5 μl . The detection limit of the qPCRs was deducted from non-
192 template controls. No amplification was detected after 45 cycles, setting the theoretical detection limit to
193 one copy L^{-1} . As the detection limit depends on the sample and elution volumes, we calculated a detection
194 limit of 40 copies L^{-1} . For *nifH* transcript diversity analysis, a PCR based amplification of the *nifH* gene
195 was performed followed by Topo TA cloning and sequencing using established protocols (Lam et al.,
196 2007;Langlois et al., 2005). Sequences were submitted to GenBank (accession numbers: KX090448-
197 KX090515).

198 Phylogenetic analysis of *nifH* transcripts was conducted using a Muscle alignment on a 321 bp fragment
199 with the Mega 6.0 package (Tamura et al., 2013), sequence differences were set at a minimum of 5%,
200 neighbor joining trees were constructed as previously described (Löscher et al., 2014).

201

202 3 Results and Discussion

203 The investigated eddies originated from the shelf-slope region of the Peru margin (however, the exact
204 origin of eddy B could not be determined). While eddy A remained close to the coast during the two

205 months period, eddies B and C propagated further offshore. Key hydrographical properties are specified
206 below but an extensive description can be found in Stramma et al. (2013).

207 **Eddy A**, a nearshore mode water eddy, showed a pronounced O₂ minimum from 100 m downwards with
208 lowest concentrations close to the detection limit of the Winkler method (~ 2 μmol O₂ kg⁻¹). The influence
209 of the coastal upwelling was visible from the lifting of the upper isopycnal towards the shore (Arévalo-
210 Martínez et al., 2015). Below the oxycline at ~ 100 m depth, nutrient concentrations were generally higher
211 in the ODZ relative to surface waters. While PO₄³⁻ concentrations were not considerably different in the
212 eddy compared to surrounding waters, NO₃⁻ concentrations showed a pronounced decrease in the ODZ of
213 eddy A compared to surrounding waters (see figure S1 for individual sections through eddies A, B and C).
214 This decrease correlated with an increase in NO₂⁻ concentrations at the same depth (r² = 0.76, n= 52 below
215 the oxycline). A comparison to biogenic N₂ as indicator for active or past N loss processes showed a
216 maximum along with the NO₂⁻ maximum thus supporting the view of ongoing N loss in eddy A (Fig. 2,
217 see Bourbonnais et al. (2015) for details on N loss processes in eddy A). As a result of this N loss, we
218 observed large values for excess P*, which is classically considered to promote N₂ fixation in surface
219 waters (Karl et al., 2002).

220 Eddy A, which was estimated to exist for two months at the time of the first survey, was sampled again
221 one month later; the first observation is further referred to as “eddy A1”, the second survey is referred to
222 as “eddy A2”. Since the first observation, a decrease in O₂ (table 1) and NO₃⁻ (Arévalo-Martínez et al.,
223 2015;Stramma et al., 2013) has been observed indicating ongoing respiration and N loss. These signals of
224 enhanced ongoing N loss weakened over time as eddy A aged (Stramma et al., 2013). An extensive
225 characterization of N loss signals in this eddy revealed a complete consumption of NO₃⁻ (Bourbonnais et
226 al., 2015), possibly due to nutrient subduction via organic matter export out of the anticyclonic eddy
227 (Omand et al., 2015). Most intense N loss signals were observed near the core of eddy A, where the ODZ
228 is in direct contact with the euphotic zone via uplifting of isopycnals (Bourbonnais et al., 2015) thus
229 supporting the impact of freshly produced organic matter on N loss (Babbin et al., 2014).

230 **Eddy B**, an offshore mode water eddy, was characterized by slightly deeper oxycline and nutriclines
231 compared to eddy A (at ~200 m water depth). Although less pronounced than in eddy A, NO₃⁻
232 concentrations decreased within the ODZ in the eddy along with an increase in NO₂⁻ and biogenic N₂
233 between 200 and 300 m depth, again indicating N loss. P* was slightly higher in the O₂ depleted core
234 waters, however, to a lesser extent and slightly deeper compared to eddy A. Stramma et al. (2013)
235 observed weaker signals for N loss in eddy B, which were also mirrored by lower N₂O production
236 (Arévalo-Martínez et al., 2015). This weakening may result from less organic matter export into the core
237 of the eddy (Fig. 2).

238 **Eddy C**, was the investigated offshore cyclonic eddy (Fig. 2) (Stramma et al., 2013). NO_3^- did not show
239 the same pronounced decrease in the core of the eddy as detected in eddies A and B, but NO_2^- and
240 biogenic N_2 were found slightly enriched between 200 and 300 m water depth, possibly from the onset of
241 N loss at this location or a left-over signal from enhanced N loss within the coastal upwelling as
242 previously described for this region (Kalvelage et al., 2013), and confirmed by the excess of P compared
243 to N in its core waters. A coastal origin of eddy C has been described; however, compared to the mode
244 water eddies A and B, eddy C moved westward without staying in the shelf/slope region (Stramma et al.,
245 2013), which may be one reason for the lower N loss signals.

246

247 **3.2 Patterns of N_2 and C fixation in the three eddies**

248 N_2 fixation was strongly associated with intermediate waters of the mode water eddies A and B, while the
249 cyclonic eddy C showed maximum rates of N_2 fixation in surface waters but no detectable N_2 fixation in
250 the O_2 depleted core waters.

251 In eddy A1, intense N_2 fixation was detected between 200 and 350 m water depth in the eddy center with
252 maximum rates of $4.4 \text{ nmol N L}^{-1} \text{ d}^{-1}$ at 250 m depth (Fig. 3). At the same depth, carbon fixation was the
253 highest reaching $0.51 \text{ } \mu\text{mol C L}^{-1} \text{ d}^{-1}$, coinciding with elevated N_2 fixation. High carbon fixation associated
254 to the center of eddy A extended, however, deeper down to 400 m. **High carbon fixation in the absence of**
255 **light (compare chl a data in Stramma et al., 2013) is likely attributed to dark carbon fixation as previously**
256 **described to take place in this and other OMZs (Schunck et al., 2013, Taylor et al., 2001).** Similarly, eddy
257 B showed high rates of N_2 fixation in its center with maxima of $1.89 \text{ nmol N L}^{-1} \text{ d}^{-1}$ at 350 m depth. In
258 eddy B, the maximum in carbon fixation was exclusively present above the upper isopycnal, and thus not
259 in direct contact with the N_2 fixation zone. However, a smaller peak could be observed at ~ 380 m depth.
260 Maximum N_2 fixation rates in eddy C ($0.51\text{-}1.48 \text{ nmol N L}^{-1} \text{ d}^{-1}$) were detected in surface waters (Table
261 S1). Carbon fixation in eddy C was lower compared to eddy A and B, however also mostly present
262 towards the rim, while close to the detection limit in the center.

263 Compared to previous studies in this area, N_2 fixation rates for eddies A and B are generally 1-2 orders of
264 magnitude higher (e.g. Dekaezemacker et al. (2013): $0.01\text{-}0.88 \text{ nmol N L}^{-1} \text{ d}^{-1}$; Löscher et al. (2014):
265 $0.01\text{-}0.4 \text{ nmol N L}^{-1} \text{ d}^{-1}$); here, it must be noted that we used the improved method by Mohr et al. (2010)
266 which allow us to present here the first quantitative rates of N_2 fixation in this area, while previous studies
267 may have underestimated N_2 fixation rates (Grosskopf et al., 2012). An aging effect was mirrored by a
268 decrease in N_2 and C fixation below 200m in the center of Eddy A when comparing the measurements
269 from eddy A1 sampled in November 2012 with eddy A2 surveyed a month later in December 2012. C
270 fixation rates increased towards the eddy edge. This may be attributed to biological consumption or export

271 of nutrients needed for biological activities within the eddy that are still available due to lower
272 consumption or diffusion through the rim.

273 Observations of higher N₂ fixation rates in accordance with our dataset suggest an overall stimulation of
274 N₂ fixation associated with anticyclonic mode water eddies (Fong et al., 2008). N₂ fixation rates of 8.6
275 nmol N L⁻¹ d⁻¹ have been measured in surface waters of an eddy in the oligotrophic North Pacific Ocean
276 (Fong et al., 2008). N₂ fixation was only measured in surface water samples (5 m depth) in Fong et al.
277 (2008), thus a direct comparison with N₂ fixation within the O₂-depleted eddy core waters, as measured in
278 this study, is not possible.

279 The occurrence of enhanced N₂ fixation associated with intermediate water depths is in accordance with
280 our previous study from that region, where we detected a variety of non-cyanobacterial diazotrophs
281 compared to relatively minor numbers of cyanobacterial diazotrophs related to *Crocospaera* (Löscher et
282 al., 2014). In order to characterize the expression of the key functional marker gene for N₂ fixation, *nifH*,
283 we conducted a phylogenetic study on *nifH* diversity in the transcript pool. Similar to the previous study,
284 most of the detected *nifH* transcripts were affiliated to non-cyanobacterial diazotrophs (P1-P8) with some
285 cyanobacterial *Crocospaera*-related (UCYN-B) *nifH* sequences present at much lesser extent (Fig. 4,
286 table S2). Quantification of *nifH* transcripts related to the detected clusters showed maximum abundances
287 associated with the maxima in N₂ fixation in eddy A, B and C (Fig. 4). A potential for heterotrophic N₂
288 fixation was deduced from glucose fertilization experiments with water samples from the cores of eddies
289 A and B. Here, glucose addition greatly enhanced N₂ fixation from 0.86 ± 0.1 nmol N L⁻¹ d⁻¹ to $39.19 \pm$
290 4.31 nmol N L⁻¹ d⁻¹ at 100 m depth in eddy A and from 0.251 ± 0.03 nmol N L⁻¹ d⁻¹ to 62.18 ± 1.9 nmol N
291 L⁻¹ d⁻¹ at 125 m depth in eddy B, respectively. However, no increase in N₂ fixation by glucose addition
292 could be achieved in eddy C (100 m, Fig. 5), which may result from different diazotrophic communities
293 (i.e. cyanobacterial UCYN-B *nifH* sequences present). Therefore, the availability of reduced carbon
294 compounds may essentially control N₂ fixation in mode water eddies. Assuming that organic matter export
295 is limiting for N loss as previously suggested (Babbin et al., 2014; Ogawa et al., 2001; Bianchi et al., 2014)
296 and that deep water N₂ fixation is a non-cyanobacterial (i.e., heterotrophic) process as shown by the
297 diversity of the diazotrophs and the stimulation of N₂ fixation rates after glucose addition, the interplay
298 between both may be even closer as previously thought.

299

300 **3.3 Co-occurrence of N₂ fixation and N loss in mode water eddies**

301 Largely consistent with the distribution of NO₂⁻, biogenic N₂ showed pronounced maxima below the
302 mixed layer depth in eddies A and B, and a less pronounced maximum in eddy C. A similar distribution
303 has been determined for P* (Fig. 2). The consistency of those parameters indicates either ongoing N loss
304 or its left-over signal as already reported for the upwelling off Peru (Kalvelage et al., 2013). In an earlier
305 study from that region (i.e., Löscher et al., 2014), we found a close spatial coupling between N loss, or a

306 relic signal as suggested by Kalvelage et al. (2013), and N_2 fixation for the same upwelling region off
307 Peru. The strongest signals for both N_2 fixation and N loss were tightly linked to a coastal sulphidic plume
308 (Schunck et al., 2013). The westward propagation of mesoscale eddies implies that properties of the
309 waters which were “trapped” within its center at the time of formation are transported offshore (Chelton et
310 al., 2007). Enhanced N_2 and C fixation rates, as well as high N deficit, as depicted by P^* , and biogenic N_2
311 concentrations in eddy B indeed suggest that this coupling can be transported far offshore.

312 A coupling between N loss and N_2 fixation is indicated by (i) the concurrent deepening of the maxima in N
313 loss (i.e. maximum in biogenic N_2) and N_2 fixation from the coast to the open ocean, (ii) the concurrent
314 decrease in both biogenic N_2 concentrations and N_2 fixation rates over time and (iii) the co-occurrence
315 between NO_2^- (either resulting from NO_3^- reduction or from remineralization of organic matter through
316 NH_4^+ oxidation) and N_2 fixation rates, and between biogenic N_2 and N_2 fixation rates (Fig. 2, 3). We
317 observed lower biogenic N_2 signals and N_2 fixation in eddy B compared to eddy A1 with the maximum in
318 N_2 fixation located deeper (~350 m) in the water column, compared to eddy A1 (~250 m). While we
319 detected enhanced carbon fixation in eddy A at the same depth as N_2 fixation, this coupling was far less
320 pronounced in eddy B. Still P^* was lower in eddy B compared to eddy A, which points towards a
321 normalization of N:P ratio *via* N_2 fixation.

322 Although, our results provide evidence for a coupling of N_2 fixation and N loss, statistical analysis of our
323 dataset, however, did not confirm N loss as exclusive control on N_2 fixation, but displays a dependence of
324 N_2 fixation on O_2 and temperature, as well (Fig. 6). The dependency on O_2 would explain the difference of
325 N_2 fixation between the modewater eddies A and B, and the cyclonic eddy C, which was in its ODZ
326 slightly less anoxic. Several studies suggested primary production to be limited by Fe availability in the
327 upwelling system off Peru (Bruland et al., 2005; Hutchins and al., 2002; Messie and Chavez, 2015). Baker
328 et al. (2015) report in their study from the same cruise series excess Fe supply (with respect to N supply)
329 via atmospheric deposition to the southern part of this region (~15-16°S). As previous studies identified
330 iron (Fe) to generally (co-)limit N_2 fixation (Mills et al., 2004; Moore and Doney, 2007; Moore et al.,
331 2009), atmospheric Fe sources may promote surface water N_2 fixation, which may explain enhanced N_2
332 fixation in surface waters of the eddies. Other studies emphasize the comparably higher importance of the
333 benthic Fe source in these waters (Chever et al., 2015; Scholz et al., 2014), which may be particularly
334 important in eddies A and B due to their longer residence time at the coast. Enhanced N_2 fixation in the
335 mode-water eddies A and B may, besides a coupling to N loss, be additionally promoted by Fe availability
336 possibly from benthic sources.

337

338 4. Conclusions

339 We conducted the first detailed survey of N₂ fixation in three eddies off the coast of Peru in the ETSP. Our
340 results demonstrated enhanced N₂ fixation rates connected to two anticyclonic mode water eddies off
341 Peru, while N₂ fixation was not increased in the cyclonic eddy. N₂ fixation rates were highest in the ODZ
342 of the two anticyclonic mode water eddies. This is in agreement with recent findings, which demonstrated
343 that N₂ fixation is not only present in oligotrophic surface waters but also widely distributed throughout
344 the water column. N₂ fixation co-occurred with N loss processes, which in combination with low O₂
345 concentrations may largely explain the presence of N₂ fixation in ODZ waters. Taken together, our results
346 point towards an important role for eddies in supplying fixed N compounds to the open ocean via
347 enhanced N₂ fixation. Although our data do not allow quantification of the overall impact of eddies on N₂
348 fixation in the ETSP off Peru, they clearly underscore the importance of high-resolution surveys for
349 understanding the biogeochemistry of N cycle processes in eddies.

350

351 Acknowledgements

352 We thank the Peruvian authorities for the permission to work in their territorial waters. We further thank
353 the captains, crews and chief scientists of R/V Meteor during the M90 and M91 cruises. We acknowledge
354 the technical assistance of T. Baustian, V. Len, V. Lohmann, N. Martogli, G. Krahnemann, K. Nachtigall,
355 M. Philippi, H. Schunck and J. Larkum. We further thank L. Stramma, D. Arevalo-Martinez, S. Thomsen,
356 C. Callbeck and J. Karstensen for helpful discussion of the results. The cruise M91 was funded by the
357 BMBF project SOPRAN with grant # FKZ 03F0662A. This study is a contribution of the DFG-supported
358 collaborative research center SFB754 (<http://www.sfb754.de>) and was supported by NSF grants OCE
359 0851092 and OCE 115474 to M.A.A. and a NSERC Postdoctoral Fellowship to A. B..

360

361

362 **References**

- 363 Altabet, M. A., Ryabenko, E., Stramma, L., Wallace, D. W. R., Frank, M., Grasse, P., and Lavik, G.: An
364 eddy-stimulated hotspot for fixed nitrogen-loss from the Peru oxygen minimum zone, *Biogeosciences*, 9,
365 4897–4908, 2012.
- 366 Arévalo-Martínez, D. L., Kock, A., Löscher, C. R., Schmitz R. A., and Bange, H. W.: Influence of
367 mesoscale eddies on the distribution of nitrous oxide in the eastern tropical South Pacific, *Biogeosciences*
368 *Discuss.*, 12, 9243-9273, doi:10.5194/bgd-12-9243-2015, 2015.
- 369 Babbin, A. R., Keil, R. G., Devol, A. H., and Ward, B. B.: Organic matter stoichiometry, flux, and oxygen
370 control nitrogen loss in the Ocean, *Science*, 344, 406-408, doi:10.1126/science.1248364 2014.
- 371 Baker, A. R., Thomas, M., Bange, H. W., and Plasencia Sánchez, E.: Soluble trace metals in aerosols over
372 the tropical south east Pacific offshore of Peru, *Biogeosciences Discuss.*, submitted, 2015.
- 373 Bianchi, D., Babbin, A. R., and Galbraith, E. D.: Enhancement of anammox by the excretion of diel
374 vertical migrators, *Proc. Natl. Acad. Sci. U. S. A.*, 111, 15653-15658, 10.1073/pnas.1410790111, 2014.
- 375 Bourbonnais, A., Altabet, M. A., Charoenpong, C. N., Larkum, J., Hu, H., Bange, H. W., and Stramma,
376 L.: N-loss isotope effects in the Peru oxygen minimum zone studied using a mesoscale eddy as a
377 natural tracer experiment., *Global Biogeochem. Cycles*, 29, doi:10.1002/2014GB005001, 2015.
- 378 Bruland, K. W., Rue, E. L., Smith, G. J., and DiTullio, G. R.: Iron, macronutrients and diatom blooms in
379 the Peru upwelling regime: brown and blue waters of Peru, *Marine Chemistry*, 93, 81-103, 2005.
- 380 Chaigneau, A., Eldin, G., and Dewitte, B.: Eddy activity in the four major upwelling systems from
381 satellite altimetry (1992-2007), *Prog. Oceanogr.*, 83, 117–123, 2009.
- 382 Chelton, D. B., Schlax, M. G., Samelson, R. M., and de Szoeke, R. A.: Global observations of large
383 oceanic eddies, *Geophysical Research Letters*, 34, doi:10.1029/2007GL030812, 2007.
- 384 Chelton, D. B., Gaube, P., Schlax, M. G., Early, J. J., and Samelson, R. M.: The Influence of Nonlinear
385 Mesoscale Eddies on Near-Surface Oceanic Chlorophyll, *Science*, 334, 328–332, 2011.
- 386 Chever, F., Rouxel, O. J., Croot, P. L., Ponzevera, E., Wuttig, K., and Auro, M.: Total dissolvable and
387 dissolved iron isotopes in the water column of the Peru upwelling regime, *Geochimica Et Cosmochimica*
388 *Acta*, 162, 66-82, doi:0.1016/j.gca.2015.04.031, 2015.
- 389 Codispoti, L. A.: Phosphorus vs. nitrogen limitation of new and export production, in: *Productivity of the*
390 *Ocean: Present and Past*, edited by: Berger, H., Smetacek, V. S., and Wefer, G., John Wiley & Sons, New
391 York, 377–394, 1989.
- 392 Codispoti, L. A.: An oceanic fixed nitrogen sink exceeding 400 Tg Na(-1) vs the concept of homeostasis
393 in the fixed-nitrogen inventory, *Biogeosciences*, 4, 233-253, 2007.

- 394 Dabundo, R., Lehmann, M. F., Treibergs, L., Tobias, C. R., Altabet, M. A., Moisaner, P. H., and
395 Granger, J.: The Contamination of Commercial $^{15}\text{N}_2$ Gas Stocks with ^{15}N -Labeled Nitrate and
396 Ammonium and Consequences for Nitrogen Fixation Measurements, *PLoS One*, 9,
397 doi:10.1371/journal.pone.0110335, 2014.
- 398 Dekaezemacker, J., Bonnet, S., Grosso, O., Moutin, T., Bressac, M., and Capone, D. G.: Evidence of
399 active dinitrogen fixation in surface waters of the eastern tropical South Pacific during El Nino and La
400 Nina events and evaluation of its potential nutrient controls, *Glob. Biogeochem. Cycle*, 27, 768-779,
401 10.1002/gbc.20063, 2013.
- 402 Deutsch, C., Sarmiento, J. L., Sigman, D. M., Gruber, N., and Dunne, J. P.: Spatial coupling of nitrogen
403 inputs and losses in the ocean, *Nature*, 445, 163-167, 10.1038/nature05392, 2007.
- 404 Duce, R. A., LaRoche, J., Altieri, K., Arrigo, K. R., Baker, A. R., Capone, D. G., Cornell, S., Dentener, F.,
405 Galloway, J., Ganeshram, R. S., Geider, R. J., Jickells, T., Kuypers, M. M., Langlois, R., Liss, P. S., Liu,
406 S. M., Middelburg, J. J., Moore, C. M., Nickovic, S., Oschlies, A., Pedersen, T., Prospero, J., Schlitzer, R.,
407 Seitzinger, S., Sorensen, L. L., Uematsu, M., Ulloa, O., Voss, M., Ward, B., and Zamora, L.: Impacts of
408 atmospheric anthropogenic nitrogen on the open ocean, *Science*, 320, 893-897, 10.1126/science.1150369,
409 2008.
- 410 Fernandez, C., Farias, L., and Ulloa, O.: Nitrogen Fixation in Denitrified Marine Waters, *Plos One*, 6, 9,
411 e20539,10.1371/journal.pone.0020539, 2011.
- 412 Fernandez, C., Gonzalez, M. L., Muñoz, C., Molina, V., and Farias, L.: Temporal and spatial variability of
413 biological nitrogen fixation off the upwelling system of central Chile (35–38.5°S), *J. Geophys. Res.*
414 *Oceans*, 120, 3330–3349, doi:10.1002/2014JC010410, 2015.
- 415 Fong, A. A., Karl, D. M., Lukas, R., Letelier, R. M., Zehr, J. P., and Church, M. J.: Nitrogen fixation in an
416 anticyclonic eddy in the oligotrophic North Pacific Ocean, *Isme Journal*, 2, 663-676,
417 10.1038/ismej.2008.22, 2008.
- 418 Friedrich, G. E., Codispoti, L. A., and Sakamoto, C. M.: Bottle and pumpcast Data from the 1988 Black
419 Sea Expedition, MBARI, Pacific Grove, Monterey, CA 93950, USA., Technical Report 1988.
- 420 Grasshoff, G., Kremling, K., Erhardt, M. : Methods of seawater analysis, 3 ed., Wiley VCH, Weinheim,
421 1999.
- 422 Grosskopf, T., Mohr, W., Baustian, T., Schunck, H., Gill, D., Kuypers, M. M. M., Lavik, G., Schmitz, R.
423 A., Wallace, D. W. R., and LaRoche, J.: Doubling of marine dinitrogen-fixation rates based on direct
424 measurements, *Nature*, 488, 361-364, 10.1038/nature11338, 2012.
- 425 Hamme, R. C., and Emerson, S. R.: Mechanisms controlling the global oceanic distribution of the inert
426 gases argon, nitrogen and neon, *Geophysical Research Letters*, 29, doi:10.1029/2002GL015273, 2002.
- 427 Hammer, Ø., Harper, D. A. T., and Ryan, P. D.: PAST: Paleontological statistics software package for
428 education and data analysis, *Palaeontologia Electronica*, 4, 9pp, 2001.

- 429 Hutchins, D. A., and al., e.: Phytoplankton iron limitation in the Humboldt Current and Peru Upwelling,
430 *Limnology and Oceanography*, 47, 997-1011, 2002.
- 431 Kalvelage, T., Lavik, G., Lam, P., Contreras, S., Artega, L., Löscher, C. R., Oschlies, A., Paulmier, A.,
432 Stramma, L., and Kuypers, M. M. M.: Nitrogen cycling driven by organic matter export in the South
433 Pacific oxygen minimum zone, *Nature Geosci*, 6, 228-234, 2013.
- 434 Karl, D., Michaels, A., Bergman, B., Capone, D., Carpenter, E., Letelier, R., Lipschultz, F., Paerl, H.,
435 Sigman, D., and Stal, L.: Dinitrogen fixation in the world's oceans, *Biogeochemistry*, 57, 47+, 2002.
- 436 Klein, P., and Lapeyre, G.: The Oceanic Vertical Pump Induced by Mesoscale and Submesoscale
437 Turbulence, in: *Annual Review of Marine Science*, *Annual Review of Marine Science*, 351-375, 2009.
- 438 Lam, P., Jensen, M. M., Lavik, G., McGinnis, D. F., Muller, B., Schubert, C. J., Amann, R., Thamdrup,
439 B., and Kuypers, M. M. M.: Linking crenarchaeal and bacterial nitrification to anammox in the Black Sea,
440 *Proc. Natl. Acad. Sci. U. S. A.*, 104, 7104-7109, 10.1073/pnas.0611081104, 2007.
- 441 Langlois, R. J., LaRoche, J., and Raab, P. A.: Diazotrophic diversity and distribution in the tropical and
442 subtropical Atlantic ocean, *Applied and Environmental Microbiology*, 71, 7910-7919,
443 10.1128/aem.71.12.7910-7919.2005, 2005.
- 444 Löscher, C. R., Großkopf, T., Desai, F., Gill, D., Schunck, H., Croot, P., Schlosser, C., Neulinger, S. C.,
445 Lavik, G., Kuypers, M. M. M., LaRoche, J., and Schmitz, R. A.: Facets of diazotrophy in the oxygen
446 minimum zone off Peru, *ISME J*, 8, 2180-2192, doi: 10.1038/ismej.2014.71, 2014.
- 447 McGillicuddy, D. J., Anderson, L. A., Bates, N. R., Bibby, T., Buesseler, K. O., Carlson, C. A., Davis, C.
448 S., Ewart, C., Falkowski, P. G., Goldthwait, S. A., Hansell, D. A., Jenkins, W. J., Johnson, R., Kosnyrev,
449 V. K., Ledwell, J. R., Li, Q. P., Siegel, D. A., and Steinberg, D. K.: Eddy/wind interactions stimulate
450 extraordinary mid-ocean plankton blooms, *Science*, 316, 1021-1026, 10.1126/science.1136256, 2007.
- 451 Messie, M., and Chavez, F. P.: Seasonal regulation of primary production in eastern boundary upwelling
452 systems, *Progress in Oceanography*, 134, 1-18, doi:10.1016/j.pocean.2014.10.011, 2015.
- 453 Mills, M. M., Ridame, C., Davey, M., La Roche, J., and Geider, J. G.: Iron and phosphorus co-limit
454 nitrogen fixation in the eastern tropical North Atlantic, *Nature*, 429, 292–294, doi: 10.1038/nature02550
455 2004.
- 456 Mohr, W., Grosskopf, T., Wallace, D. W. R., and LaRoche, J.: Methodological underestimation of oceanic
457 nitrogen fixation rates, *PLoS One*, 5, e12583, 2010.
- 458 Montoya, J. P., Voss, M., Kahler, P., and Capone, D. G.: A simple, high-precision, high-sensitivity tracer
459 assay for N₂ fixation, *Applied and Environmental Microbiology*, 62, 986-993, 1996.
- 460 Moore, J. K., and Doney, S. C.: Iron availability limits the ocean nitrogen inventory stabilizing feedbacks
461 between marine denitrification and nitrogen fixation, *Global Biogeochem. Cycles*, 21,
462 doi:10.1029/2006GB002762, 2007.

463 Moore, M. C., Mills, M. M., Achterberg, E. P., Geider, R. J., LaRoche, J., Lucas, M. I., McDonagh, E. L.,
464 Pan, X., Poulton, A. J., Rijkenberg, M. J. A., Suggett, D. J., Ussher, S. J., and Woodward, E. M. S.: Large-
465 scale distribution of Atlantic nitrogen fixation controlled by iron availability, *Nature Geosci*, 2, 867-871,
466 2009.

467 Ogawa, H., Amagai, Y., Koike, I., Kaiser, K., and Benner, R.: Production of refractory dissolved organic
468 matter by bacteria, *Science*, 292, 917–920, doi:10.1126/science.1057627, 2001.

469 Olson, E. M., McGillicuddy, D. J., Flierl, G. R., Davis, C. S., Dyrman, S. T., and Waterbury, J. B.:
470 Mesoscale eddies and *Trichodesmium* spp. distributions in the southwestern North Atlantic, *J. Geophys.*
471 *Res. Oceans*, 120, doi:10.1002/2015JC010728, 2015.

472 Omand, M. M., D'Asaro, E. A., Lee, C. M., Perry, M. J., Briggs, N., Cetinić, I., and Mahadevan, A.:
473 Eddy-driven subduction exports particulate organic carbon from the spring bloom, *Science* 348,
474 doi:10.1126/science.1260062, 2015.

475 Scholz, F., McManus, J., Mix, A. C., Hensen, C., and Schneider, R. R.: The impact of ocean
476 deoxygenation on iron release from continental margin sediments, *Nature Geoscience*, 7, 433-437, 2014.

477 Schunck, H., Lavik, G., Desai, D. K., Großkopf, T., Kalvelage, T., Löscher, C. R., Paulmier, A.,
478 Contreras, S., Siegel, H., Holtappels, M., Rosenstiel, P., Schilabel, M. B., Graco, M., Schmitz, R. A.,
479 Kuypers, M. M. M., and LaRoche, J.: Giant Hydrogen Sulfide Plume in the Oxygen Minimum Zone off
480 Peru Supports Chemolithoautotrophy, *PLoS ONE*, 8, 2013.

481 Sohm, J. A., Webb, E. A., and Capone, D. G.: Emerging patterns of marine nitrogen fixation, *Nat Rev*
482 *Micro*, 9, 499-508, 2011.

483 Stramma, L., Bange, H. W., Czeschel, R., Lorenzo, A., and Frank, M.: On the role of mesoscale eddies for
484 the biological productivity and biogeochemistry in the eastern tropical Pacific Ocean off Peru,
485 *Biogeosciences*, 10, 7293-7306, doi:10.5194/bg-10-7293-2013, 2013.

486 Tamura, K., Stecher, G., Peterson, D., Filipowski, A., and Kumar, S.: MEGA6: Molecular Evolutionary
487 Genetics Analysis Version 6.0, *Molecular Biology and Evolution*, 30, 2725-2729, 2013.

488 Taylor GT, Iabichella M, Ho TY, Scranton MI, Thunell RC, et al. (2001) Chemoautotrophy in the redox
489 transition zone of the Cariaco Basin: A significant midwater source of organic carbon production. *Limnol*
490 *Oceanogr* 46: 148–163. doi: 10.4319/lo.2001.46.1.0148

491 Warembourg, F. R.: Nitrogen fixation in soil and plant systems, in: *Nitrogen Isotope Techniques*, edited
492 by: Knowles, R., and Blackburn, T. H., Academic Press, San Diego, USA, 127-156, 1993.
493
494
495

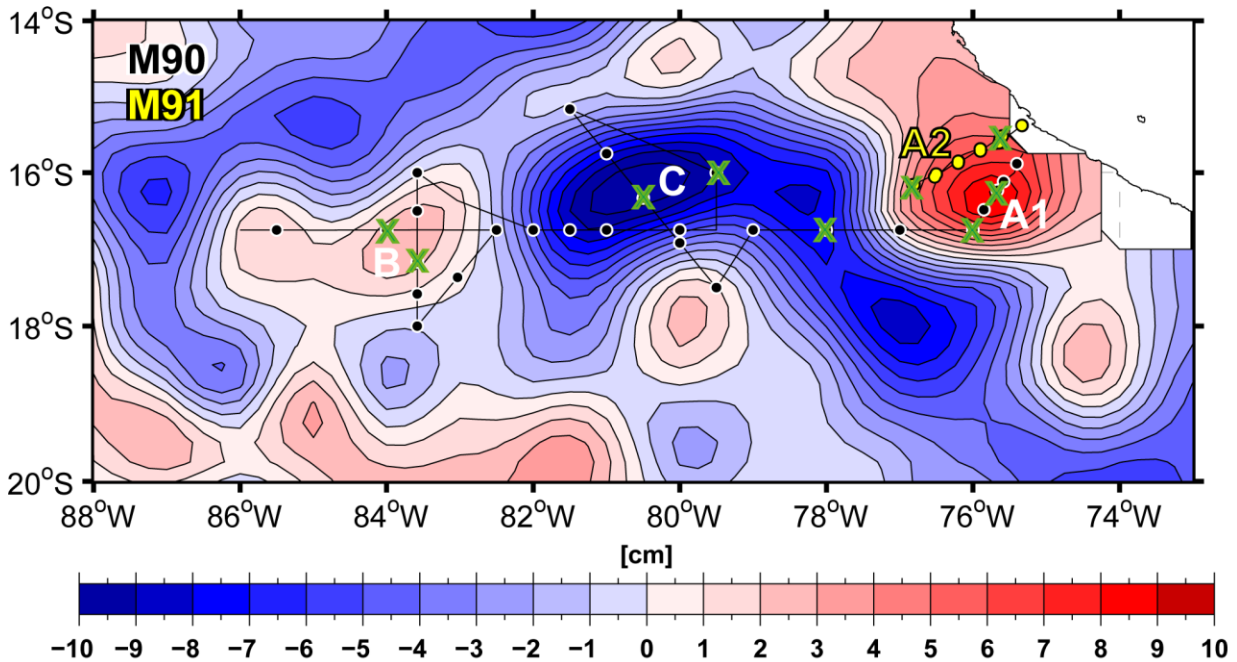
496 **Tables**

497 Table 1. Vertically integrated biogeochemical **parameters** of the three eddies in the ETSP during the M90
 498 and M91 cruises. N₂ and C fixation rates as well as O₂ concentrations are expressed as integrated
 499 concentrations/abundances over the upper 500 m of the water column (data taken from the eddy centers).
 500 Chl *a* concentrations are taken from Stramma et al. (2013) and represent maximum concentrations in the
 501 subsurface maximum.

	A (M90)	A (M91)	B (M90)	C (M90)
N ₂ fixation (μmol N m ⁻² d ⁻¹)	628.7	490.8	245.0	150.6
C fixation (mmol C m ⁻² d ⁻¹)	64.4	3.9	42.8	6.7
O ₂ (mol m ⁻²)	37.5	27.6	37.7	45.2
chl <i>a</i> max. (μg L ⁻¹)	6.1	2.5	2.5	2.8

502

503 **Figures**

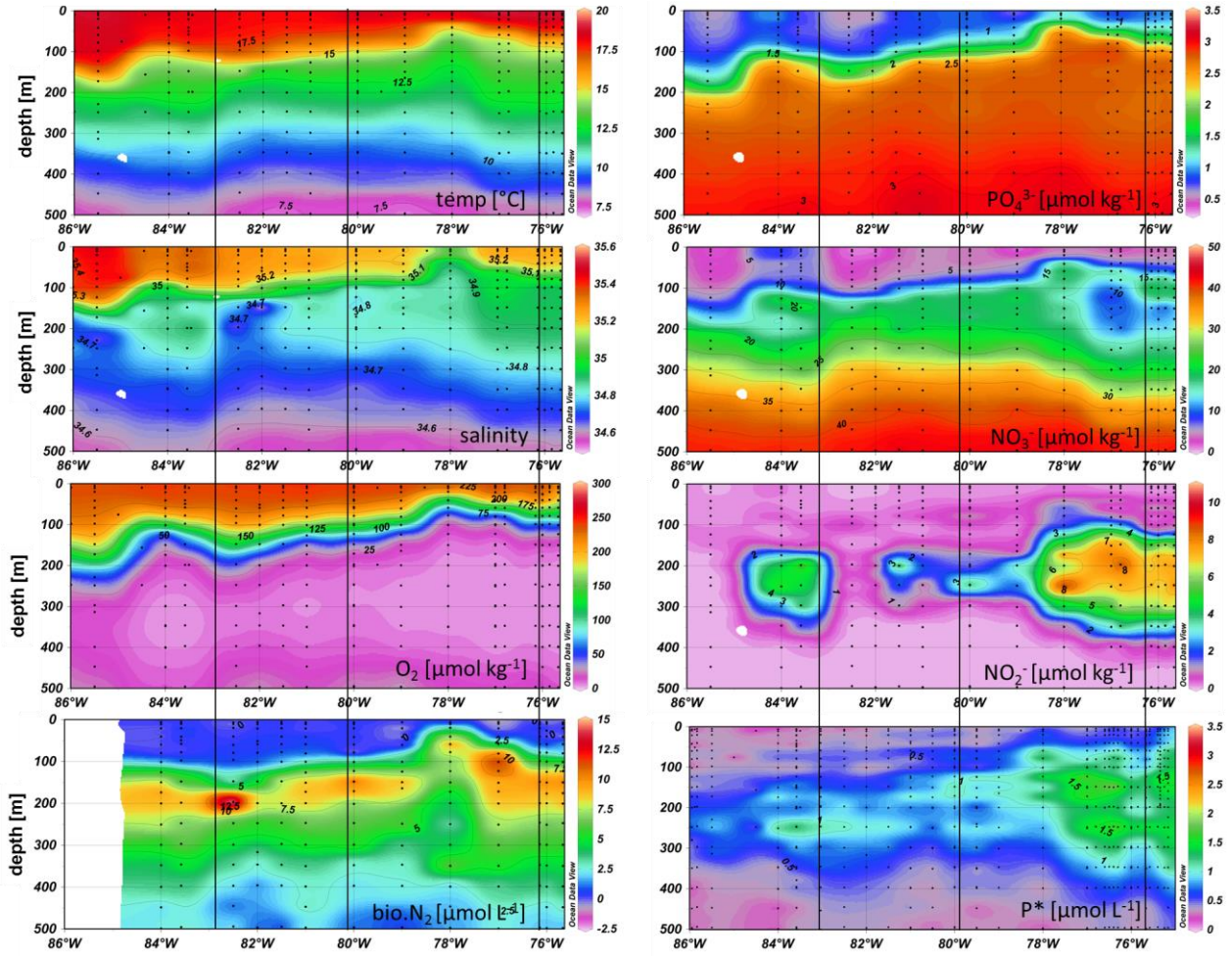


504

505 Figure 1: Distribution of **Aviso satellite-derived sea surface height anomaly (SSHA)** distribution as
 506 described by Stramma et al. (2013) on 21 November 2012. Eddies are labelled in white (A and B denote
 507 the coastal and the open ocean mode water eddies, respectively; C denotes the cyclonic eddy). The cruise
 508 track from the M90 cruise is shown in black, CTD-bottle stations are indicated with black dots, green

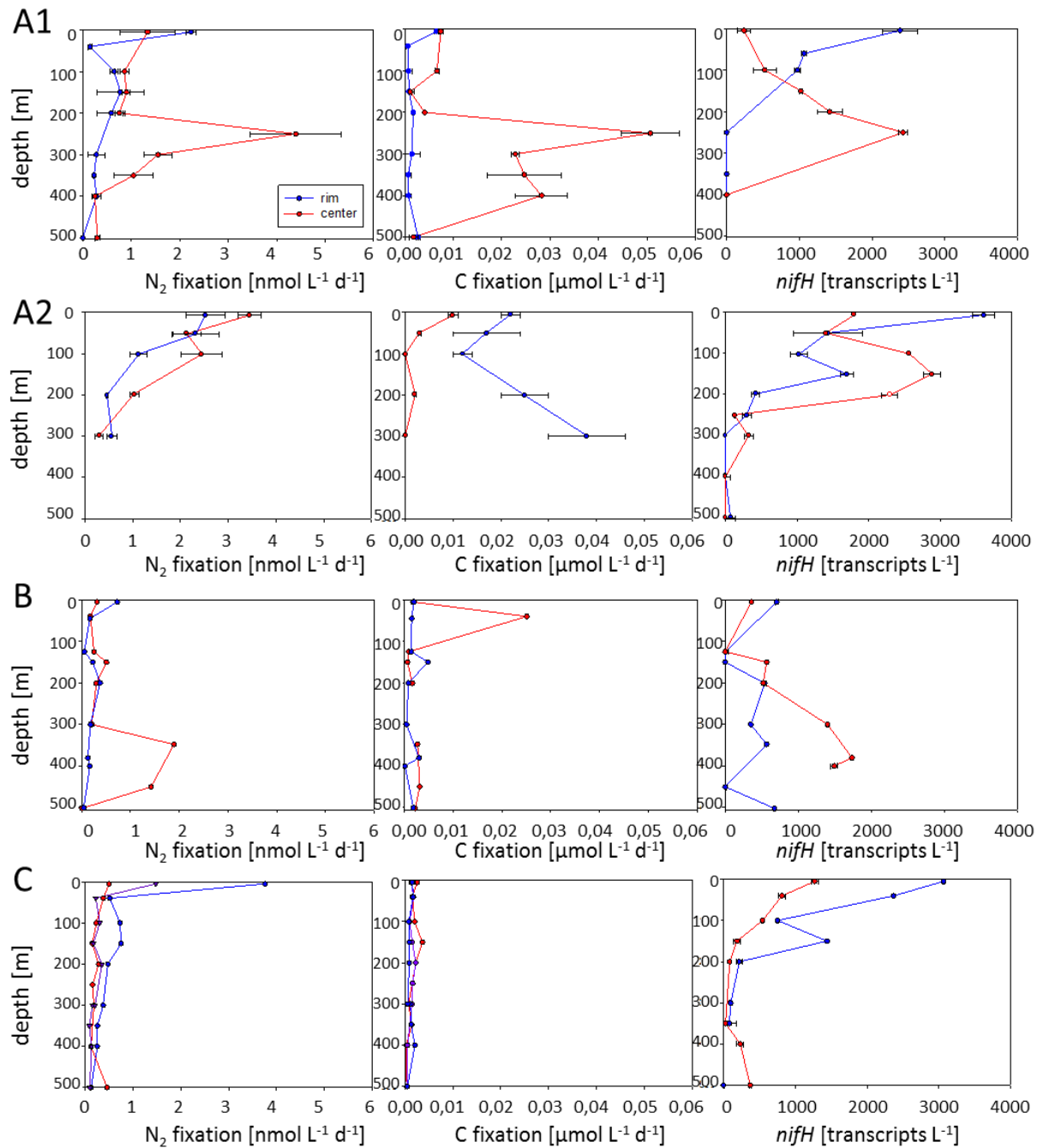
509 crosses denote stations sampled for N₂ fixation. The cross section through the aged coastal mode water
 510 eddy during the consecutive cruise M91 is denoted with yellow dots (A2).

511



512
 513 Figure 2: Temperature, salinity and oxygen, phosphate, nitrate, nitrite, biogenic N₂ and P* for eddies A, B
 514 and C along a cross section at 16°45'S during the M90 cruise are shown. The black lines indicate the eddy
 515 centers at ~76°W (eddy A), ~80.1°W (eddy C) and ~83.3°W (eddy B).

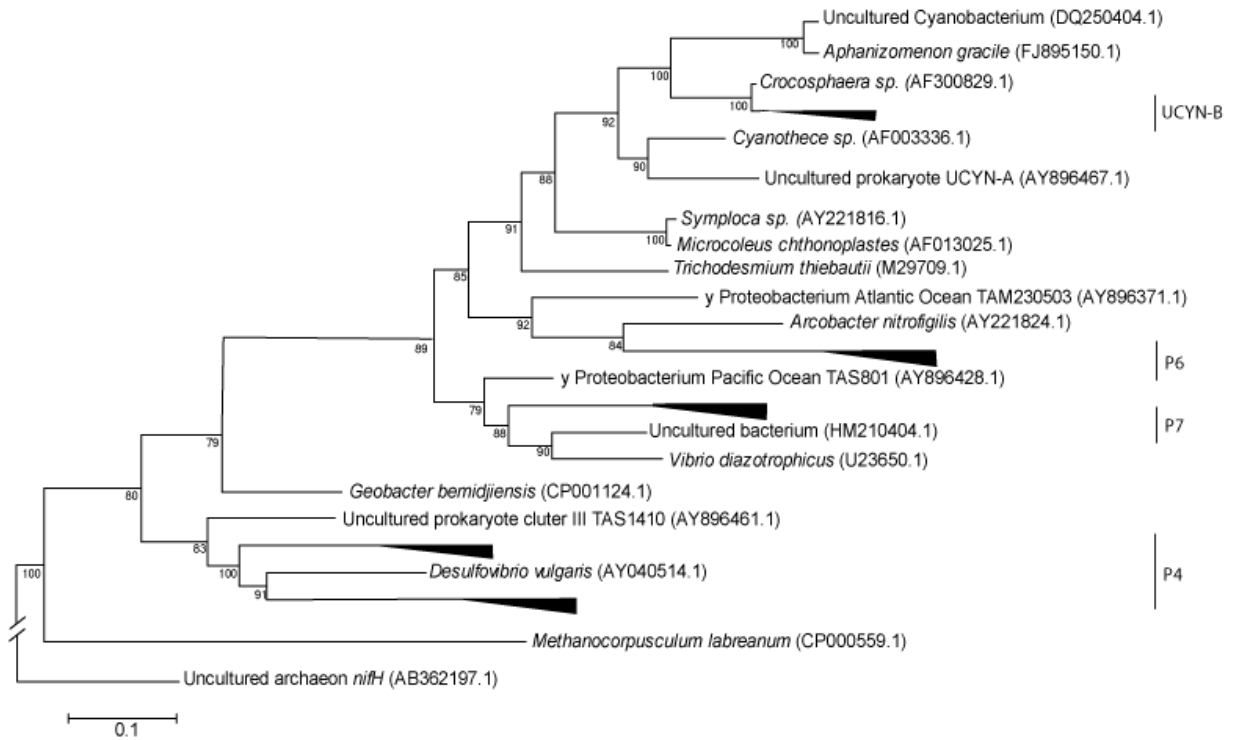
516



517

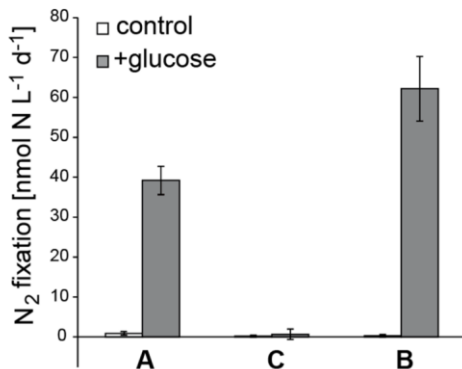
518 **Figure 3:** Vertical distributions of N_2 and C fixation rates and *nifH* transcript abundance (sum of detected
 519 clusters P2, P7 and *Crocospaera*-like diazotrophs as quantified by qPCR) in eddy A1 (M90), eddy A2
 520 (M91), eddy B and eddy C.

521



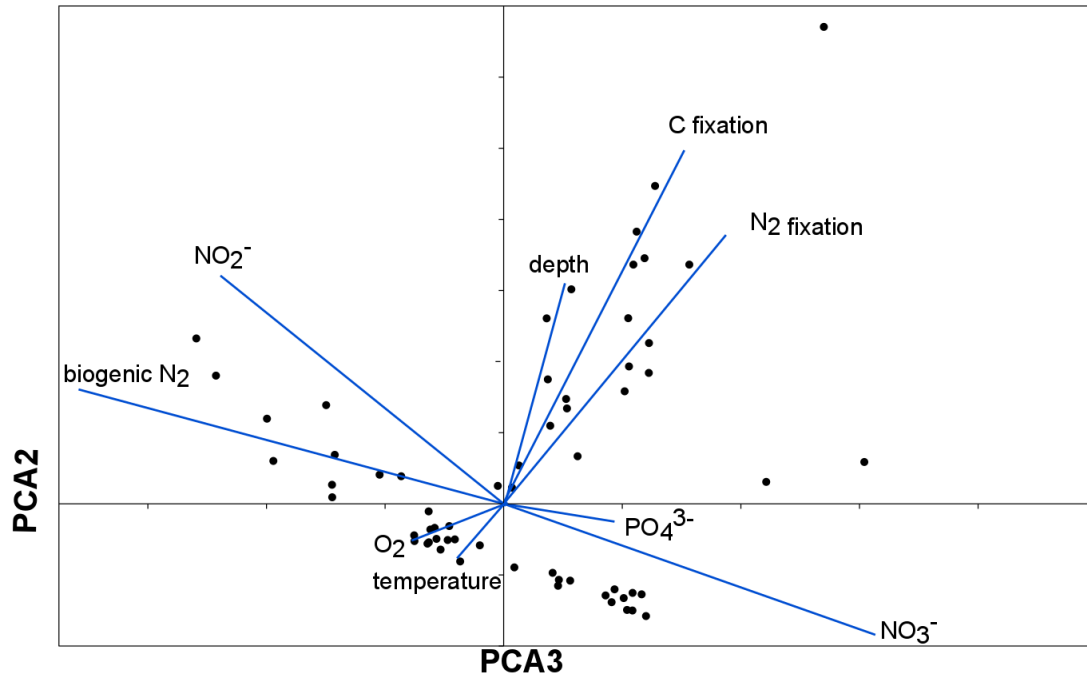
522
 523 Figure 4: Phylogenetic diversity in *nifH* cDNA libraries, black triangles denote detected clusters present in
 524 samples from M90 and M91. The tree was constructed from a ClustalW alignment as a neighbor joining
 525 tree, bootstrap values are given (% of 1000 bootstraps) below branches, P4, P6 and P7 are clusters
 526 previously identified in that region (Löscher et al., 2014).

527



528
 529 Figure 5: N₂ fixation in response to glucose fertilization experiment performed in eddy **AI** (100 m), B
 530 (125 m) and C (100 m); samples were derived from the eddy center stations water depth.

531



532

533 Figure 6: Principal component analysis correlation biplot shows relations between N₂ fixation and
 534 environmental variables. Strongest negative correlations are present between N₂ fixation and O₂ and N₂
 535 fixation and **temperature**. N₂ fixation is positively correlated with C fixation as indicated by the direction
 536 of vectors. Black dots denote single samples (n=58).